International Journal for Holistic Research, Vol. 2, No. 2. Jan 2025

OPEN ACCESS
Print ISSN: 3009-6898
Online ISSN: 3009-6790

Analysis of zebra optimization method for sizing optimum design of wind turbine-photovoltaic-fuel cell HRES

Mohammed Morad [1], Doaa A. Gad [2,3*], Ahmed A.M. El Gaafary[3], Adel A. Elbaset[4], Mokhtar Said[5]

[1] Electrical Engineering and Computers Engineering Dep., Higher Institute of Engineering and Technology, New Minya, Egypt;

[2] Electrical Engineering Department, Future High Institute of Engineering, Fayoum 63511, Egypt.

[3] Electrical Engineering Department, Faculty of Engineering, Minia University, El-Minia, Egypt

[4] Department of Electromechanics ,Engineering, Faculty of Engineering, Heliopolis University, Cairo, Egypt.

[5]Electrical Engineering Department, Faculty of Engineering, Fayoum University, Fayoum 43518, Egypt.

* Correspondence : Doaa A. Gad, doaagad.pg@eng.s-mu.edu.eg

Article history: Received: 23-07-2024 Revised: 15-09-2024 Accepted: 17-10-2024

Abstract

This paper presents an optimized design for a photovoltaic-wind turbine-fuel cell (PV-WT-FC) hybrid renewable energy system (HRES) aimed at fulfilling the power demands of both industrial facilities and residential buildings in the Egyptian city of Siwa. The primary PV-WT system offers an economical approach to power distribution, with any surplus energy efficiently channeled to an electrolyzer, which generates hydrogen. In instances where generated power falls short, the stored hydrogen is utilized by a proton exchange membrane fuel cell (PEMFC), ensuring a continuous and smooth supply of electricity to the load. Consequently, fuel cells act as supplementary sources designed to mitigate power fluctuations and provide a stable electricity supply. The Zebra optimization algorithm (ZOA) is employed to determine the optimal configuration of the proposed HRES, with the results being compared to those obtained from the cuckoo search algorithm (CSA). The optimization problem's objective is to minimize both the loss of power supply probability (LPSP) and the cost of energy (COE), which includes the number of PV arrays and wind turbines as decision variables. The findings indicate that the optimal HRES configuration includes 82 PV arrays, 113 wind turbines, and 150 fuel cells.

Keywords: PV;WT;Optimization; ZOA; LPSP; COE

.

1. Introduction

Developing renewable energy sources is crucial for transforming energy systems and reducing greenhouse gas emissions [1]. Global pollution decreased by 5.9% in 2020 due to the coronavirus epidemic, significantly reducing energy consumption and shifting attention towards hybrid renewable energy systems (HRES) [2]. These systems integrate one or more renewable energy sources (RE) to enhance system efficiency and reliability. Various energy sources, including fuel cells (FCs), wind, biomass, solar, hydropower, and biogas, are combined in these systems. FCs are particularly valued for their high efficiency, surpassing that of batteries [3-7]. The vast majority of HRESs operate independently or in combination with electrical grids, with stand-alone systems commonly used in remote areas to meet local energy demands [8]. The shift towards HRESs has been driven by the need for a more stable power supply and a more flexible energy system. These systems offer the ability to connect supply and load demand, as well as transmit electricity to remote regions. This is especially important as the demand for power continues to grow, and traditional power plants struggle to meet these requirements [9-17].

Recently, several studies suggested techniques for optimal hybrid systems' size providing more reliability with lower costs [18-22]. In the literature, F. S. Mahmoud et al. (2022) [23] present optimal sizing of photovoltaic-wind turbine-fuell cell (PV-WT-FC) using Marine Predators' algorithm and Seagull Optimization algorithm with run accounting for the uncertainty in load demand. R. J. Rathish et al. (2021) [24] use strong Pareto evolutionary algorithm that demonstrate the best way to combine PV, WT, and diesel energy sources to minimize CO2 emissions and acquire the lowest possible overall cost of a hybrid system. A. Maleki et al. (2015) [25] introduce best design of a solar-wind system with a storage battery bank by applying the genetic algorithm to minimize the loss of power supply probability (LPSP) and the overall cost of the system. M. J. Hadidian-Moghaddam et al. (2016) [26] use grey wolf optimization to adopt the best design for a PV-WT-battery hybrid system to reduce total annual cost and increase system reliability. M. Bilal et al. (2022) [27] show three hybrid energy system configurations to meet the power needs of the electric

Cite this article: Mohammed Morad, et. al.” Analysis of zebra optimization method for sizing optimum design of wind turbine-photovoltaic-fuel cell HRES “, International Journal for Holistic Research, Vol. 2, No. 2. Jan 2025. DOI: 10.21608/ijhr.2024.306650.1024

vehicle charging station that is in India's northwest that are: (a) PV-diesel generator-battery based electric vehicle charging station, (b) PV-battery based electric vehicle charging station, and (c) grid-PV based electric vehicle charging station. The optimization algorithm aims to minimize the total net present cost and levelized cost of energy, all while ensuring that the value of the probability of power supply shortages remains within specified limits. C. Ghenai et al. (2020) [28] FCs have drawn increased attention as storage devices and have been crucial to HRES in providing load with continuous power. A. A. Z. Diab et al. (2019) [29] apply four novel optimization algorithms of Water Cycle Algorithm, Whale Optimization Algorithm, Hybrid particle swarm-gravitational search algorithm, and Moth-Flame Optimizer to design optimal PV-WT-diesel-battery hybrid system with minimum cost of energy (COE) and LPSP. Sultan et al. (2021) [30] the suggested IAEO algorithm shows quick convergence properties, the best objective function minimum values, and the lowest EC compared to the traditional AEO, PSO, SSA, and GWO algorithms. Khan and Javaid (2020) [31] the PV/FC is the most cost-effective hybrid system
compared to the PV/WT/FC and WT/FC systems. The Jaya method's results showed its superiority compared to other algorithms used. Duman and Güler (2018) [32] this system presented the dispatch control strategies and the optimal ratings of the renewable system units. According to the techno economic analysis of this study, showed that battery storage is still economically superior to hydrogen storage. Hadidian Moghaddam et al. (2019) [33] FPA method showed the best results in solving the optimal sizing problem with fast convergence, minimum Total NPC and better reliability compared to the other optimization algorithms used. PV/WT/FC system is the most cost-effective for many situations, with lower costs and higher reliability indices in comparison to other suggested hybrid system combinations.

The literature review makes clear the primary focus of the researchers is on hybrid renewable energy systems and their optimal sizing. Motivated by the literature review considerations, the main objectives and contributions of this work are:

• Optimal PV/WT/FC HRES for residential housing and industrial units in the Egyptian city of Siwa has been designed.
• A novel new metaheuristic technique known as the Zebra algorithm, it incorporates the best features of a lot of other algorithms, it has been used to address the optimization issue. The size number of PV arrays, WTs, are used as choice variables in the optimization problem. On the other hand, the fitness function is the LPSP minimization and estimated the number of FCs.
• The energy analysis cost for the ideal system size has been established, The system saved 87.7% from cost compared cost without HRES.
• We have analyzed the performance of the Zebra approach by examining its resilience and convergence curves through statistical analysis of 100 independent runs.
• To prove the optimal effective and performance of the ZOA methodology, the results of ZOA are compared with re compared with other optimization algorithms.
• Applied the Sensitivity analysis of ZOA algorithm for two cases covering the system for 100% and 50% of load demand in three configurations (PV/FC, WT/FC and PV/WT/FC).

The paper is structured as follows: Section 2 will delve into the modeling of the hybrid system, following the introduction. The methodology, described in section 3, will then be introduced, followed by the clarification of Zebra algorithm process in section 4. The discussion on the application and results is introduced in section 5. Finally, section 6 presents the conclusion.

2. Modeling of PV-WT-FC hybrid system

The content modeling of PV/WT/FC is depicted in Figure 1. The system includes an AC bus and a DC bus. The consumer's energy interests are met through the utilization of energy generated from PV and WTs, which are dual sources. Any residual energy is directed to an electrolyzer to generate hydrogen, which is stored in a hydrogen tank for later use in fueling a fuel cell. In instances where the generated power falls short of meeting the demand for load, the fuel cell is responsible for feeding the load. The HRES parameters are presented Table 1, which contain the rated power for PV, WT, FC, electrolyzer and converter, also Open circuit voltage
Short circuit current.

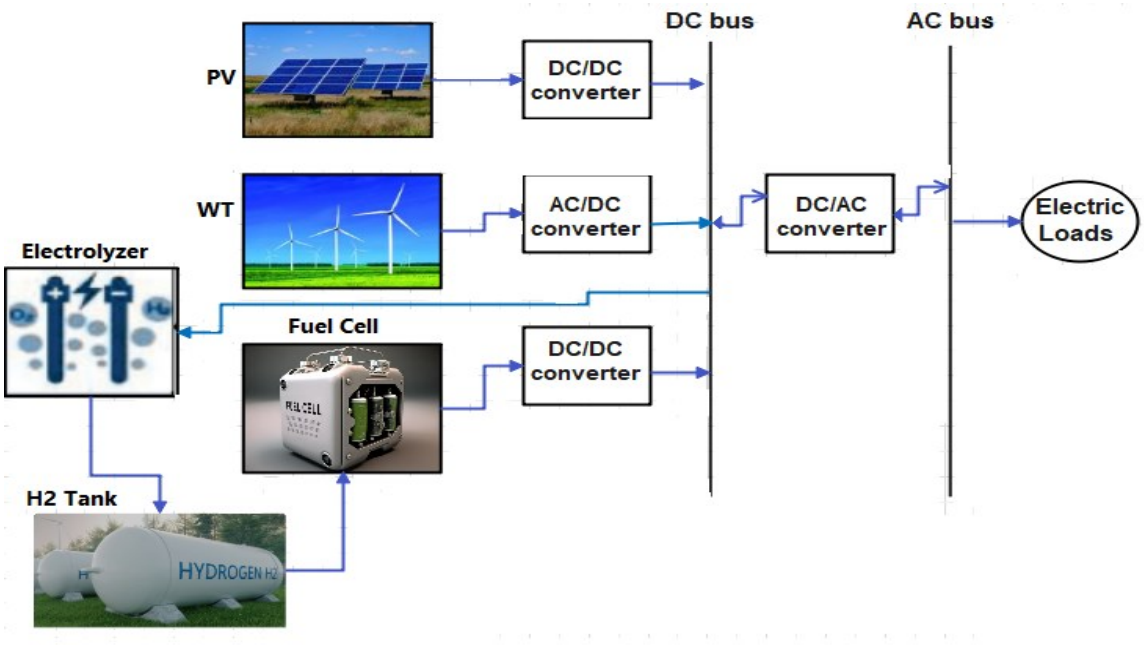

Fig. 1. PV/WT/FC hybrid system

Table 1. Comparing the results obtained from protection schemes with other works

Component	Parameters	Value
PV array	Panel model	BBS24MF400 (Mono PERC)
	Maximum power	400 W
	Open circuit voltage	50.49 V
	Short circuit current	9.98 A
WT	Model	REYAH - H50
	Rated power	50 kW
	Beginning wind speeds	3 m/s
	Wind speed rated.	10 m/s
	Surviving wind speed	50 m/s
	Wheel diameter	17.6 m
FC	Model	Fuel cell stack EH-81
	Rated power	100kW
	Voltage range	231-513 V
	Peak current	450A
	Efficiency	85 %
Electrolyzer	Model	PEM
	Rated power	300 kW
	Voltage	415 V
	Efficiency	75 %
Converter	Rated power	150 kW
	Efficiency	90 %

2.1. Modeling of PV system

The PV system output energy (PV_E) is given by [38]:

$$\mathrm{PV_E} = \frac{\mathrm{S_{Glo}}}{\mathrm{S_{Stand}}} \times \mathrm{N_{PV}} \times \mathrm{P_{PVr-cap}} \times \mathrm{f_{de\_pv}} \quad (1)$$

Where; S_{Glo} is the worldwide incident solar radiation (kWh/m^2), S_{Stand} is standard solar radiation (1 kWh/m^2), $P_{PVr-cap}$ is PV array rated capacity (kW), f_{de_pv} is PV array derating factor, N_{PV} is the number of PV arrays.

2.2 Modeling of WT system

The output power of the wind turbine generator varies with changes in wind speed, which, in turn, depends on the height at the same site. Figure 2 shows the power output of the wind turbine generator at the hub height as a function of wind speed. The wind speed (V) at the turbine hub height h (meter) is given by [3],

$$V = V_o \left(\frac{h}{h_o}\right)^{0.142} m/s \quad (2)$$

The WT generated power (P_{WT}) is calculated as follows [3], [23],

$$P_{WT} = \begin{cases} N_{WT} * v^3 * \dfrac{P_r(1 - {v_{cut-in}}^3)}{{v_r}^3 - {v_{cut-in}}^3} & v_{cut-in} \le v < v_r \\ N_{WT} * P_{WT_r} & v_r \le v < v_{cut-out} \\ 0 & otherwise \end{cases} \quad (3)$$

Where, N_{WT}: the number of wind turbines, v : wind speed (m/s), v_{cut-in}: cut-in wind speed (m/s), $v_{cut-out}$: cut-out wind speed (m/s), v_r: rated wind speed (m/s).

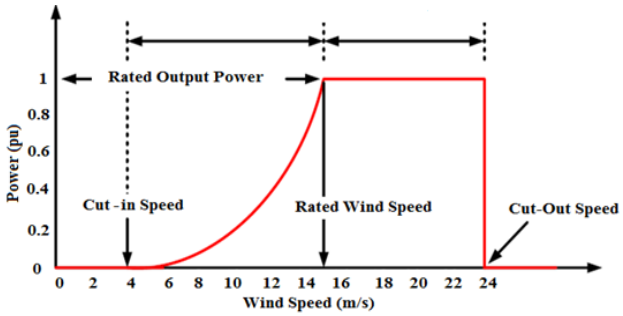

Fig.2. Wind speed with power.

2.3 Modeling of Electrolyzer

By running a direct current (DC) across double electrodes to separate water into hydrogen (from anode side) and oxygen (from cathode side), the electrolyzer to produce hydrogen s fueled by the excess energy created by PVs and wind sources (See Equation (5)). Subsequently, the hydrogen generated is kept in high-pressure tanks [23].

$$Electricity + H_2O = H_2 + \frac{1}{2}O_2 \quad (4)$$

The following equation shows power output that is moved from the electrolyzer into the hydrogen tank [23].

$$P_{out-ele} = P_{in\_ele} \times \tau_{ele} \quad (5)$$

Where $P_{out-ele}$ electrolyzer's power output (kw), P_{in_ele} power input (kw),τ_{ele} electrolyzer's constant efficiency.

2-4. Modeling of H_2Tank

When power output from wind and PV resources is low during peak hours, FCs are fed the necessary amount of hydrogen to make up for any shortage in the needed power. The following is an illustration of energy from hydrogen in any (t) [23]:

$$E_{tank_{H_2}}(\Delta t) = E_{tank_{H_2}}(t-1) + (P_{out-ele} - \frac{P_{\sup\_fc}(t)}{\tau_{tank}} \times \Delta t \quad (6)$$

Where; $E_{tank_{H_2}}(\Delta t), E_{tank_{H_2}}(t-1)$ are energy stored in tank in t and (t − 1) times, $P_{\sup\_fc}(t)$ power given to FCs, τ_{tank} is the efficiency of the hydrogen tank, is assumed to be 95% during all operations.

The next estimate is capable of being used for determining the mass of hydrogen produced by the electrolyzes. [23]:

$$M_{ank_{H_2}}(\Delta t) = \frac{E_{tank_{H_2}}(\Delta t)}{HHV} \quad (7)$$

Where;

HHV represent hydrogen's higher heating value, which is 39.7 kWh/m^2.

2-5. Modeling of FC

An electrolyzer is used for converting chemical energies to electrically DC energy in a fuel cell, which is made up of two electrons (anode and cathode) and an electrolyte. In addition to being simpler, requiring less maintenance, and having a higher efficiency than batteries, it is also a green energy source that produces no pollutants [41-43].
Equation (8) can be used to calculate the power generated by FC in the following manner and number of fc can be calculated form equation (9) [22]:

$$P_{out\_fc}(t) = P_{\sup\_fc}(t) \times \tau_{fc} \quad (8)$$

$$N_{fc} = \frac{\max(P_{fc})}{P_{fc\_rated}} \quad (9)$$

Where; τ_{fc} is FC efficiency.

2-6. Modeling of DC/AC Converter

Since the loads require alternating current (AC) power, the electricity generated by PVs and wind turbines is required to convert DC to AC power. Equation (10) is utilized to compute the inverter's output power [23].

$$P_{out\_invr} = \left(P_{out\_fc}(t) \times P_{gen}\right) \times \tau_{invr} \quad (10)$$

Where;
P_{gen} is quantity of power produced by RES.
τ_{invr} is efficiency to inverter taken to be constant at 90%.

3. Methodology

3-1. Objective function

This work seeks to identify the optimal combination of system components to maximize the HRES's energy output, while minimizing the COE and LPSP. The solution will be derived from decision variables subject to constraints as outlined below "which represents the search boundaries of the model parameters"

- **Bounds constraint**

$$N_{PV}^{min} \le N_{PV} \le N_{PV}^{max} \quad (11)$$

$$N_{WT}^{min} \le N_{WT} \le N_{WT}^{max} \quad (12)$$

Where N_{PV} is the number of PV arrays; N_{WT} is number of wind turbines, N_{PV}^{min}, N_{PV}^{max}, $N_{WT}^{min}$and N_{WT}^{max} represent the low and high boundaries of the PV and WT system which between 1: 250.
The generated power must be constrained to avoid charging problems from the electrolyzer and discharging by the FC device.

$$M_{tank_{H_2\_min}} \le M_{tank_{H_2}}(t) \le M_{tank_{H_2\_max}} \quad (13)$$

where $M_{tank_{H_2\_min}}$ represents the lowest hydrogen tanks and $M_{tank_{H_2\_max}}$ represents full capacity of H2 tanks.

3-2. LPSP

LPSP stands for the probability of encountering an inadequate power supply when a hybrid system falls short of meeting the load demand. To determine the LPSP value, the following equation is utilized,

$$\mathrm{LPSP} = \frac{\mathrm{P_{load}} - \mathrm{P_{generated}}}{\mathrm{P_{load}}} = \frac{\mathrm{P_{load}} - (\mathrm{P_{PV}} + \mathrm{P_{Wt}} + \mathrm{P_{fc}})}{\mathrm{P_{load}}} \quad (14)$$

The power generated from WT is denoted by P_{Wt}, the power generated from PV by P_{PV}, the overall amount generated power by $P_{generated}$, the load power byP_{load} and P_{fc} is the power of fuel cell.

3-3. COE

The annual overall cost of the hybrid system equals the sum of the total costs associated with the PV arrays, FCs, electrolyzer, hydrogen tank, WTs, and conversion components of the proposed system [23].

$$C_{t\_an} = C_{ca_{an}} + C_{re\_an} + C_{o\_m\_an} \quad (15)$$

Where;
C_{t_an} is the combined system's total yearly cost.
$C_{ca_{an}}$ is the annual capital cost of each system component.
C_{re_an} is the replacement annual cost.
$C_{o\_m\_an}$ is annual maintenance and operating costs for every system component.

- The calculation for annual capital cost is as follows:

$$C_{ca_{an}} = C_{ca_{an\_pv}} + C_{ca_{an\_wt}} + C_{ca_{an\_fc}} + C_{ca_{an\_ele}} + C_{ca_{an\_h2}} + C_{ca_{an\_invr}} \quad (16)$$

The cost of each individual component in the entire system for one year is depicted in equation (17).

$$\begin{bmatrix} C_{ca_{an_{pv}}} = C_{ca_{pv}} \times CRF(i, L_{pv}) \\ C_{ca_{an_{wt}}} = C_{ca_{wt}} \times CRF(i, L_{wt}) \\ C_{ca_{an_{fc}}} = C_{ca_{fc}} \times CRF(i, L_{fc}) \\ C_{ca_{an_{ele}}} = C_{ca_{ele}} \times CRF(i, L_{ele}) \\ C_{ca_{an_{h2}}} = C_{ca_{h2}} \times CRF(i, L_{h2}) \\ C_{ca_{an_{invr}}} = C_{ca_{invr}} \times CRF(i, L_{invr}) \end{bmatrix} \quad (17)$$

where starting capital costs of the PV module, FC, hydrogen tanks, electrolyzers, wind turbine module, and converter. are denoted by the letters $C_{ca_{wt}}$, $C_{ca_{fc}}$, $C_{ca_{ele}}$, $C_{ca_{h2}}$, $C_{ca_{pv}}$, and $C_{ca_{invr}}$ correspondingly. The lifetimes of PV module, hydrogen tanks, FCs, electrolyzers, WTs, and converter are, in order, L_{wt}, L_{fc}, L_{ele}, L_{h2}, L_{pv}, and L_{invr}. The annual interest rate is denoted by i.
The investment cost is converted to the capital cost using the Capital Recovery Factor (CRF). To calculate CRF, equation (18) is considered.

$$CRF(i, L_i) = \frac{i(1+i)^{L_i}}{i(1+i)^{L_i} - 1} \quad (18)$$

- Annual replacement cost: this expense arises when the component lifetime is less than the project lifetime.

$$\mathrm{C_{re\_an}} = \mathrm{C_{re\_i}} \times \frac{(\mathrm{L} - \mathrm{L_i})}{\mathrm{L}} \quad (19)$$

- Annual operation and maintenance costs: These are the expenses incurred when a hybrid system component needs to be repaired or when it is necessary to operate a component.

$$\mathrm{C_{o\_m\_an}} = \mathrm{C_{o\_m\_an\_pv}} + \mathrm{C_{o\_m\_an\_wt}} + \mathrm{C_{o\_m\_an\_fc}} + \mathrm{C_{o\_m\_an\_ele}} + \mathrm{C_{o\_m\_an\_h2}} + \mathrm{C_{o\_m\_an\_invr}} \quad (20)$$

The formula below is used to compute. COE of hybrid power systems:

$$\mathrm{COE} = \frac{\mathrm{C_{t\_an}}}{\mathrm{P_{load}}} \quad (21)$$

3.4 Operation Strategy

The operation strategy used in the proposed hybrid system is simplified in a flowchart shown in Figure 3, a HRES is designed to generate power for Siwa Osias in Egypt from solar and wind energies, with excess power being directed to an electrolyzer system to produce hydrogen. This hydrogen is stored in tanks and then used in fuel cells (FCs) to generate electricity when the generated power does not meet load demand. To achieve the best possible system sizing, several key elements need to be optimized: the size of hydrogen tanks, the number of PV arrays and wind turbines, and the rated power of FCs, inverters, and electrolyzers. These factors are interdependent, requiring a careful balance to ensure the system can reliably meet load requirements while minimizing production energy costs. A novel metaheuristic algorithm called the Zebra optimization algorithm is developed to determine the optimal sizes for PV arrays, wind turbines, and fuel cells by considering them as variables in the optimization problem. The objective is to minimize the LPSP and COE.

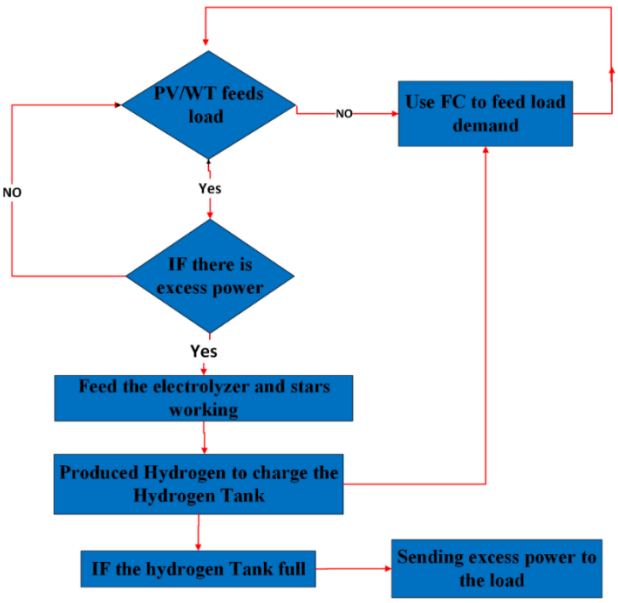

Fig.3. Operation Strategy.

4. Zebra optimization algorithm

Zebra optimization algorithm (ZOA) basic idea behind is to simulate the social behavior found in zebra herds in the natural [44]. A pioneer zebra facilitates the movement of other zebras towards the food source during the hunting technique. Consequently, a pioneer zebra leads a group of other zebras over the plains. The zebras' main defense against predation is to flee in a zigzag manner. But occasionally, they try to scare or confound the predator by congregating. The proposed ZOA design draws its fundamental inspiration from mathematical modelling of these two forms of intelligent zebra behaviors.

4.1. ZOA mathematical model

4-1-1. initialization

Zebras are part of the ZOA population, a population-based optimizer. Each Zebra is a potential remedy for the problem from a mathematical perspective, and the plain where the zebras are located is the problem's search space. The decision variables values are established by each zebra's location inside the search space. As a result, a vector may be used to describe each zebra as a member of the ZOA, with the values of the issue variables being represented by the vector's elements. A matrix can be applied to numerically model the population zebra [44]. The zebras' starting locations inside the search area are chosen at random. The population matrix for ZOA can be found in (22).

$$Z = \begin{bmatrix} Z_1 \\ \vdots \\ Z_i \\ \vdots \\ Z_N \end{bmatrix}_{N\times m} = \begin{bmatrix} z_{1,1} & \cdots & z_{1,j} & \cdots & z_{1,m} \\ \vdots & \ddots & \vdots & \ddots & \vdots \\ z_{i,1} & \cdots & z_{i,j} & \cdots & z_{i,m} \\ \vdots & \ddots & \vdots & \ddots & \vdots \\ z_{N,1} & \cdots & z_{N,j} & \cdots & z_{N,m} \end{bmatrix}_{N\times m} \quad (22)$$

Where;
N is number of individuals in a population (zebras).
m is choice variables 'number.
Z is population zebra.
z_i is ith zebra.
$z_{i,j}$ is the answer for jth problem variable provided by ith zebra.
Each zebra represents a potential solution to the optimization problem. Consequently, the proposed values of each zebra for the issue variables may be utilized to evaluate the objective function. By utilizing equation (23), the values are provided as a vector acquired for the objective function.

$$F = \begin{bmatrix} F_1 \\ \vdots \\ F_i \\ \vdots \\ F_N \end{bmatrix}_{N\times 1} = \begin{bmatrix} F(Z_1) \\ \vdots \\ F(Z_i) \\ \vdots \\ F(Z_N) \end{bmatrix}_{N\times 1} \quad (23)$$

Where;
F is vector objective function value.
F_i is objective function value acquired for ith zebra.

The best candidate solution for given issue is found by comparing the obtained values for the goal function, which effectively analyses quality of their associated candidate solutions. The zebra with lowest objective function value is the best possible solution to reduction problems. On the other hand, the optimal candidate zebra in maximization issues is the one with the greatest value of the objective function. The perfect solution for the candidate must be found in each iteration as the zebras' locations and, as a result, the values of goal function, are modified in each iteration.
ZOA members have been updated using two of the zebra's natural behaviors. The first of these two behavioral patterns is foraging, and the second is predator defense mechanisms. Participants within the ZOA community are therefore updated twice every cycle.

4-1-2. Phase 1: Foraging Behavior

Using models of zebra behavior while foraging, population members are updated in the initial phase. The plains zebra, one of the zebra species, offers habitat to other species that require shorter and more nutrient-rich grasses below. The best zebra in the population is known as the pioneer zebra in ZOA, and it guides other zebras in the population towards its location in the search space [44]. Therefore, equations (24) and (25) may be used to mathematically

simulate how zebras' positions are updated through the hunting period.

$$z_{i,j}^{new,P1} = z_{i,j} + r.\left(PX_j - I.x_{i,j}\right) \quad (24)$$

$$Z_i = \begin{cases} Z_i^{new,P1} & F_i^{new,P1} < F_i \\ Z_i & else \end{cases} \quad (25)$$

Where;

PX is the best member to represent the pioneer zebra.

PX_j is jth dimension.

r is a random number within a specific range [0; 1].

4-1-3. Phase 2: Defense Strategies Against Predators

The second step involves updating the position of ZOA population members in the search space using models of the zebra's defense mechanism against predator assaults. The mode S1 in equation (26) can be used to simulate this tactic. When a zebra is attacked by another predator, the remaining zebras in the herd migrate towards it to create a protective structure that will intimidate and confuse the attacker. The mode S2 in equation (26) is used to mathematically represent this zebra technique. Zebras update their positions, and if a new site has a greater value for the goal function, the zebra is allowed for the update. Equation (27) is used to simulate this updating circumstance.

$$z_{i,j}^{new,P2} = \begin{cases} S_1: x_{i,j} + R.(2r-1) & \\ \left(1 - \frac{t}{T}\right).x_{i,j} & P_s \le 0.5 \\ S_2: x_{i,j} + r.\left(AZ_j - I\right).x_{i,j} & else \end{cases} \quad (26)$$

$$Z_i = \begin{cases} Z_i^{new,P2} & F_i^{new,P2} < F_i \\ Z_i & else \end{cases} \quad (27)$$

Where;

$Z_i^{new,P2}$ is the updated status of the ith zebra in accordance with the second phase. $z_{i,j}^{new,P2}$ is the value of the jth dimension. $F_i^{new,P2}$ is objective function's value. t is contour of iteration. T is the biggest number of used iterations. R is constant value represents 0.01. P_s is the probability of selecting one of two randomly generated strategies in the interval [0; 1]. AZ is the assaulted zebra's status.

4-1-4. Applied ZOA algorithm

The population members are updated depending on the first and second phases at the end of each ZOA cycle. Up to the algorithm's complete implementation, the algorithm population is updated depending on equation (24) to (27). Through several cycles, the best candidate solution is updated and stored. ZOA presents the top contender as the best answer to the given problem when it has been completely developed. In Figure 4, the ZOA processes are displayed as flowcharts.

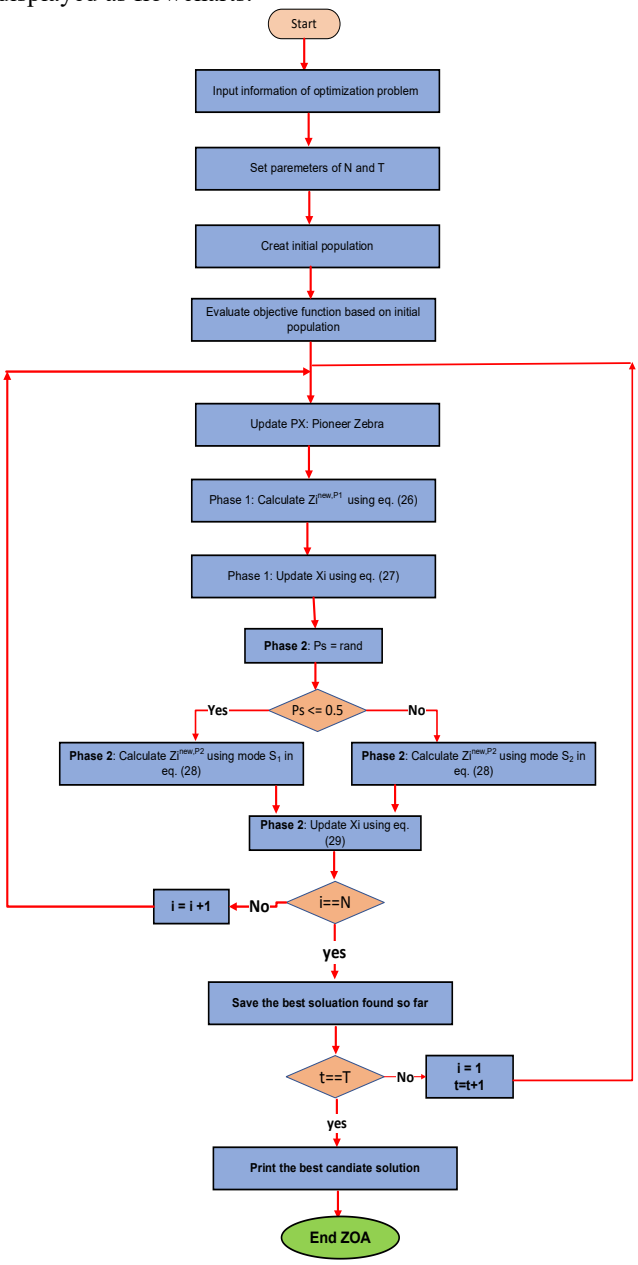

Fig.4. Flowchart of ZOA.

5. Application and results analysis

5-1. Meteorological data of case study

This study takes into consideration a specific services site in the Egyptian Oasis Siwa (29.150 N, 25.539 E). The capacity and continuity of the energy supply are limited since the facility is connected to a low-reliability electrical system. The location offers the following services: manufacturing, farms, and schools and the loads which are used in them. In Table 2, the load data is displayed. The average load profile used in each hour through 24 hours in the month July, the month which has the max load demand

100MW in the Siwa oasis is shown in Figure 5. The total loads in the site a connected load of 103 MW, the maximum load is around 100 MW.

Table 2. Load data.

Load data of schools			
Device	**Power (W)**	**Quantity**	**Total load power (MW)**
Lighting	100	43000	4.3
Appliances (class A "200 W")	2000	2000	4
Appliances (class B "100 W")	1000	5000	5
Appliances (class C "75 W")	750	4000	3
Appliances (class D "70 W")	700	1000	0.7
Appliances (class E "50 W")	500	4000	2
Load data of farms			
Device			**Power (MW)**
Total power of operating devices			24
Load data of factories			
Device			**Power (MW)**
Total power of operating devices			60

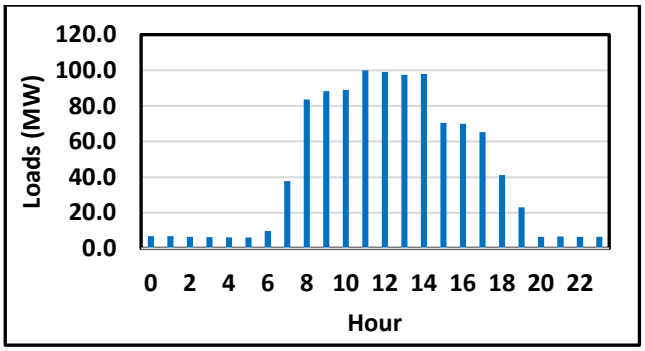

Fig. 5. Average hourly load profile through the year.

NASA's Ground Meteorological and Sun Energy webpage was consulted for site's local resources, which included temperature, wind speed, and sun radiation [45]. The average monthly sun radiation for the entire year is shown in Figure 6 and the month January has the lowest radiation with 3.732 kWh/m2/day but the month June has the biggest of radiation. At 8.43 kWh/m^2/day, June has greatest every day's average radiation from the sun and average annual solar radiation is 5.92 kWh/m^2/day. The median every month temp for the entire year is shown in Figure 7. The average annual temperature is 21.1 °C, which may have an impact on photovoltaic efficiency. Consequently, the high ambient temperature of 29.68 °C in July may have a detrimental effect on the power generation of PV panels. The monthly average wind speed at 50 meters over the ground's surface is depicted in Figure 8 for the whole year. Within median yearly speed wind of 5.53 m/s, this region offers a lot of potential for using wind energy.

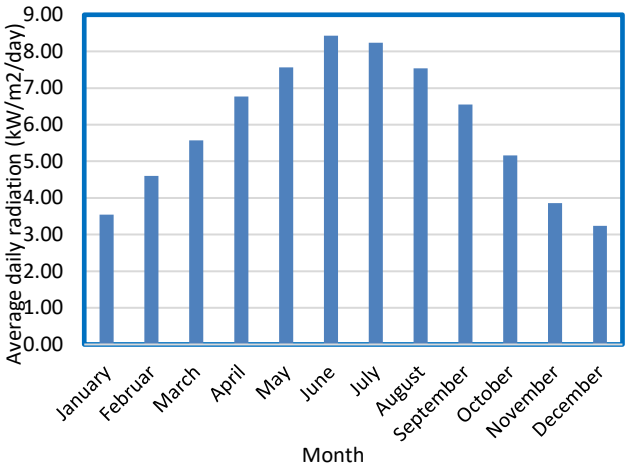

Fig. 6. Average monthly solar radiation.

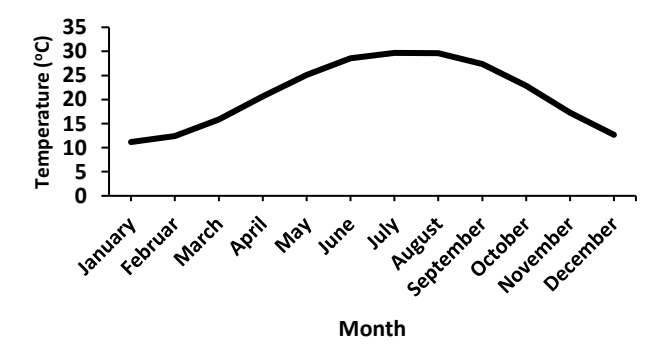

Fig.7. Average monthly temperature.

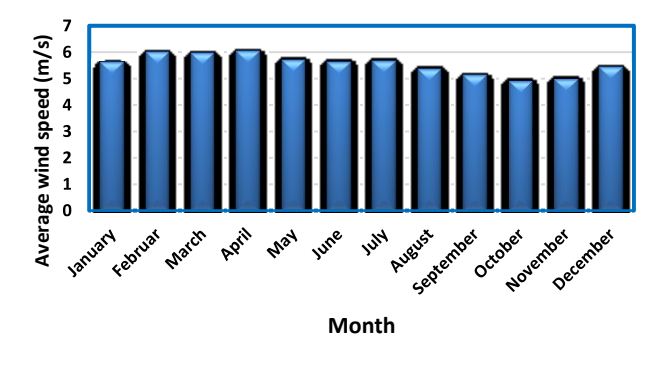

Fig.8. Average monthly wind speed.

5-2. Discussion of case study results

Table 3 provides the specs of all elements used in HRES in this investigation. The lifetime of the system was estimated to be 25 years, the interest rate to be 6%, and the FC lifetime to be 5 years.

MATLAB software is utilized to simulate and apply the suggested sizing strategy, considering significant variations in the average solar radiation, the average temperature, and the average wind speed. The model takes temperature, wind speed, and sun radiation observed data from the Oasis Siwa site as input. The number of PV arrays and WTs, which are the decision variables, have minimum and maximum constraints of 1 and 250, respectively.

Furthermore, the largest number of agents searching is 30, and the maximum is 1000 iterations. To determine the best option for each component such as size of solar PV, WTs and FCs. Table 4 presents outcomes simulation of suggested technique for two strategies. ZOA achieved the best optimum solution concluded that predicts the best COE of 0.0005712 \$/kWh, and lowest NPC = 1.1296×10^7 \$ and LPSP=0 compare with CSA algorithm estimates 0.0006439 \$/kWh to the COE and NPC = $2.41 \times 10^7$and LPSP = 5.2963×10^{-9}. But when we compare with another new algorithm, Find the ZOA achieve the best optimum solution where COE of 0.0005712 \$/kWh, and lowest NPC = 1.1296×10^7 \$ and LPSP=0 and the result of RIME algorithm COE of 0.0002562 \$/kWh, and NPC = 1.6793×10^7 \$ and LPSP=1.2963×10^{-23}.

According to the ZOA optimization algorithms, it has been demonstrated that the proposed location offers the lowest COE. After careful analysis, it has been determined that the ideal configuration for the system contain of 82 arrays PV, 113 wind turbines, 150 FCs, electrolytes rated 300 kW of power, H2 tanks with a maximum mass of 150 kg, an inverter with a rated output of 150 kW and a 100 kW-rated FC and get maximum power produced by 20 MW hydrogen production electricity by electrolysis. This optimized setup ensures efficient operation and harnesses renewable energy sources to their fullest potential.

Figures cover several aspects of the MATLAB replication and enhancement. Figure 9 shows the greatest power generated by the PV (143 MW) and wind (3.96 MW) for the month of July, which is the month with the highest load in our area. Figure 10 shows discrepancy among power and load produced by wind and photovoltaic systems; the load may produce up to 100 MW of power.

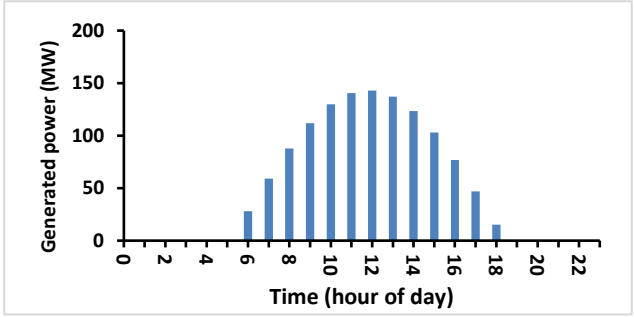

(a)

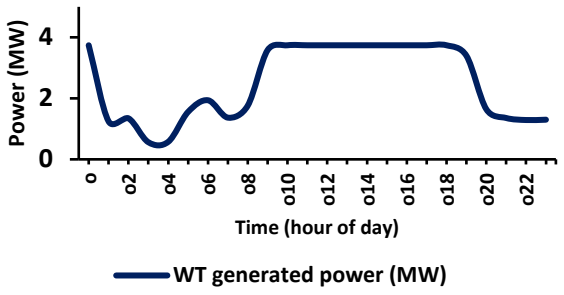

(b)

Fig. 9. Power generated from: (a) PV system, (b) WTs.

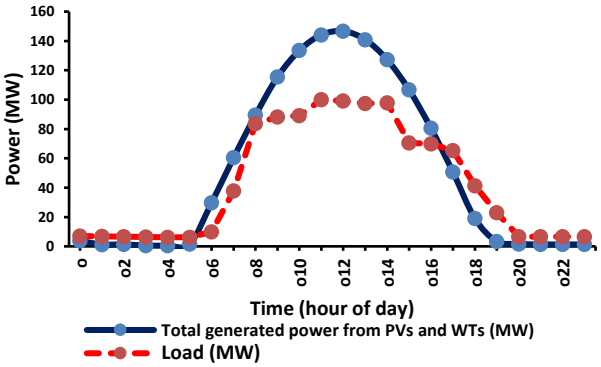

Fig.10. Power generated from PV, WT and Load demand.

If combination electrical power produced by WT and PV solar cell array exceeds the demand from the load, the electrolyzer is utilized to make hydrogen by absorbing excess energy, which is then collected in its tanks. The FC generates energy to make up for the energy shortage during low power generation hours. Figure 11 indicates the power of electroyzer and Figure 12 indicate the power of FC.

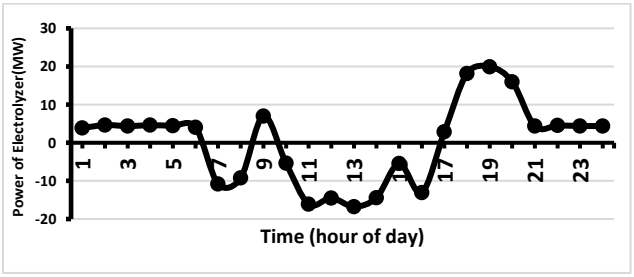

Fig 11. Power of Electrolyzer.

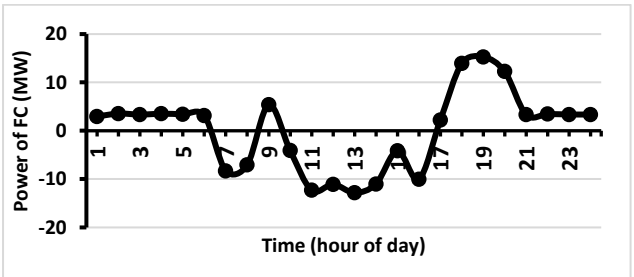

Fig.12. Power of FC.

The convergence of the Zebra algorithm throughout 100 separate runs of finding the best solutions for FC /WT/ PV HRES is depicted on Figure 13. When the best solution is achieved, which is reached by the 81st iteration, the convergence is done at random and stabilizes. There are 153 FCs, 92 WTs, and 82 PV arrays in the optimized HRES.

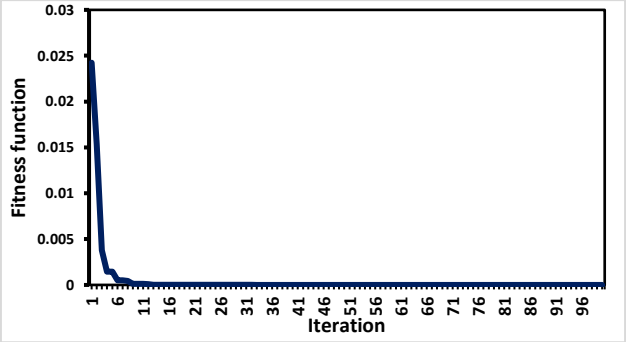

Fig.13. Convergence characteristics of Zebra algorithm.

5-3. Short-term exploration for economic feasibility of 100% renewable fraction

Considering that the fraction of energy delivered to the load originating from the designed HRES is 100% (100% renewable fraction), a short-term exploration of economic feasibility over a five-year period is being analyzed. This analysis is set up with an assumption of a 5% increase in load demand and a 1% increase in COE every year. As a result, five scenarios are established as follows:

- Scenario 1 (reference scenario): Year 2024 with 836251.5 MWh, 0.0005712 $/kWh COE for 100% renewable fraction, and 0.0390 $/kWh COE for 0% renewable fraction.
- Scenario 2: Year 2025 with 878064.1 MWh, 0.0005769 $/kWh COE for 100% renewable fraction, and 0.0394 $/kWh COE for 0% renewable fraction.
- Scenario 3: Year 2026 with 921967.3 MWh, 0.0005827 $/kWh COE for 100% renewable fraction, and 0.0398 $/kWh COE for 0% renewable fraction.
- Scenario 4: Year 2027 with 968065.6 MWh, 0.0005885 $/kWh COE for 100% renewable fraction, and 0.0402 $/kWh COE for 0% renewable fraction.
- Scenario 5: Year 2028 with 1016468.9 MWh, 0.0005944 $/kWh COE for 100% renewable fraction, and 0.0406 $/kWh COE for 0% renewable fraction.

Figure 14 illustrates the COE for annual load demand over a five-year period, from 2024 to 2028, with no renewable energy fraction. Conversely, Figure 15 presents the COE for annual load demand with a renewable energy fraction of 100% over the same five-year span.

Table 3. Economic data regarding the components of the system [23].

Elements	Wind Turbine	PV Array	Electrolyzer	Hydrogen Tank	Fuel Cell	Inverter
Cap. cost ($/unit)	118,412	136,912	52,311	17,004	71,219.2	12,387
Rep. cost ($/unit)	52,500	---------	22,500	9000	50,000	7500
O&M cost ($/unit)	5250	5000	7500	2250.4	17,500	1203,02
Lifetime (year)	20	25	20	20	5	15

Table 4. Outcomes of optimum performance values according to ZOA and CSA.

Parameter	best Solution		
	ZOA	**CSA**	**RIME**
N_PV	82	78	99
N_WT	113	240	198
N_FC	150	139	170
COE($/kWh)	0.0005712	0.0006439	0.0002562
NPC ($)	1.1296×10^7	2.41×10^7	1.6793×10^7
LPSP	0	5.2963×10^{-9}	1.2963×10^{-23}
Number of iterations to get optimum solution	81	40	77

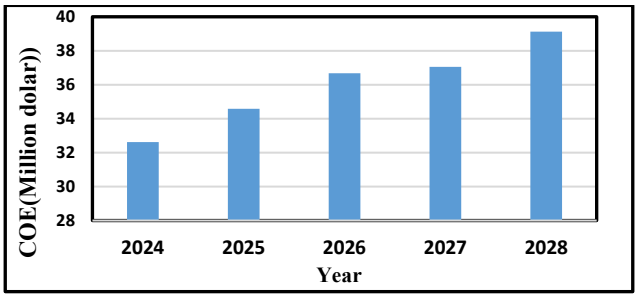

Fig. 14. COE for annual load demand with 0% renewable fraction.

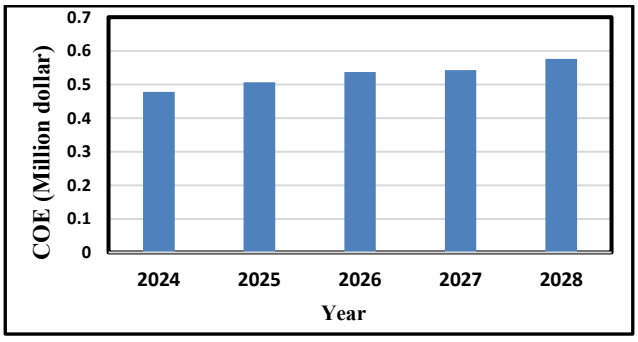

Fig. 15. COE for annual load demand with 100% renewable fraction.

In the year 2024, the cost of the COE for annual load demand decreased from 32,613,808.5 $ with no renewable fraction to 477,666.9 $ with a 100% renewable fraction. Similarly, in 2025, the COE for annual load demand saw a further reduction from 34,586,943.9 $ with no renewable fraction to 506,565.7 $ with 100% renewable fraction. By the year 2026, the COE for annual load had dropped even further, from 36,679,454 $ with no renewable fraction to 537,212.9 $ with 100% renewable fraction. Continuing the trend, in 2027, the COE for annual load demand experienced another decrease, this time from 38,898,561 $ with no renewable fraction to 569,714.3 $ with 100% renewable fraction. Finally, in the year 2028, the COE for annual load demand reached its lowest point, dropping from 41,251,923.9 $ with no renewable fraction to 604,182 $ with 100% renewable fraction.

Based on these results, it is evident that with a renewable energy fraction of 100%, the COE for annual load demand is reduced by 98.5 % each year. Over the five-year period, the total financial savings, considering the NPC of 1.1296×10^7 $, amounts to 92.4%.

5-4. Sensitivity analysis

A sensitivity analysis has been performed to assess the effects of three distinct HRES configurations on LPSP and associated costs. The configurations examined include PV/WT/FC, PV/FC, and WT/FC systems. This analysis was conducted at two different HRES penetration levels relative to the peak load demand of 100 MW, specifically at 100% and 50% penetration during July, which experiences the highest load demand in Siwa Oasis. Simulations were executed using the ZOA methodology, with results detailed in Table 5.

Table 5. Sensitivity analysis results.

Case 1: Results of system design with 100% HRES penetration ratio (100 MW)						
HRES configuration	**Number of components**			**LPSP**	**NPC ($)**	**COE ($/kWh)**
	PV	**WT**	**FC**			
PV/WT/FC	82	113	150	0	1.1297×10^7	0.0005712
PV/FC	85	-	178	0.1155×10^{-4}	1.0875×10^7	0.000755
WT/FC	-	400	528	0.85×10^{-3}	4.6857×10^7	1.006078
Case 2: Results of system design with 50% HRES penetration ratio (50 MW)						
HRES configuration	**Number of components**			**LPSP**	**NPC ($)**	**COE ($/kWh)**
	PV	**WT**	**FC**			
PV/WT/FC	24	71	38	1.44×10^{-16}	3.4652×10^6	1.001669
PV/FC	42	-	66	1.1486×10^{-10}	1.0535×10^6	0.0003924
WT/FC	-	167	10	0	1.928×10^7	5.006363

In Case 1, characterized by a 100% HRES penetration ratio, the PV/WT/FC system demonstrated the lowest LPSP and the minimum COE. Additionally, its NPC was found to be lower than that of the WT/FC system but higher than that of the PV/FC system, thereby identifying the PV/WT/FC configuration as the optimal solution. In Case 2, which

involved a 50% HRES penetration ratio, the PV/FC system emerged as the most economically favorable design, exhibiting the lowest NPC and COE values. Although the LPSP for the PV/FC system was lower than that of the PV/WT/FC system and higher than that of the WT/FC system, it still qualified as the optimal system design.

6. Conclusion

A novel approach utilized optimize the fuel cell sizing, solar, and wind components of a hybrid renewable energy system (HRES) that is linked to a stand-alone micro grid system. The month of July was picked as the case study to address energy requirements of Siwa, Egypt's residential and industrial buildings. The month with the highest load demand is July. The proposed approach aimed to reduce the Cost of Energy (COE) with high efficiency to meet the load demand according to the results of a novel metaheuristic method called the Zebra algorithm. Out of all the optimization results, the suggested zebra method also provides the ideal HRES component sizes to reduce the COE as effectively as possible while meeting load requirement.

The above proposed algorithms are applied to size and optimize the desired hybrid electrical system for supplying a residential load demand. The results show that:

- The method achieved the goal of work, minimum cost with good performance.
- A comprehensive comparison between ZOA and CSA is presented to obtain the optimal case. The simulation results ensure the superiority of ZOA in solving the optimization problem and reaching the best optimum solution of the objective function of 0.1565, which represents the minimum values of the COE of 0.0005712 $/kWh, NPC of 1.1296×10^7 and LPSP of zero, which agree with the predefined values.
- Based on these results, it is evident that with a renewable energy fraction of 100%, the COE for annual load demand is reduced by 98.5 % each year. Over the five-year period, the total financial savings, considering the NPC of 1.1296×10^7 $, amounts to 92.4%.
- In Case 1, characterized by a 100% HRES penetration ratio, the PV/WT/FC system demonstrated the lowest LPSP and the minimum COE. Additionally, its NPC was found to be lower than that of the WT/FC system but higher than that of the PV/FC system, thereby identifying the PV/WT/FC configuration as the optimal solution.
- In Case 2, which involved a 50% HRES penetration ratio, the PV/FC system emerged as the most economically favorable design, exhibiting the lowest NPC and COE values. Although the LPSP for the PV/FC system was lower than that of the PV/WT/FC system and higher than that of the WT/FC system, it still qualified as the optimal system design.

To reduce costs even further, consider using a different type of backup energy in future projects rather than batteries. Furthermore, the suggested approach may be used for various study scenarios spanning the entire year. Then, further algorithms could yield the best design for any study situation.

References

[1] S. M. Tatar, H Akulker, H Sildir, E Aydin. Optimal design and operation of integrated microgrids under intermittent renewable energy sources coupled with green hydrogen and demand scenarios, International Journal of Hydrogen Energy, 47 (2022), 27848-27865.

[2] S. S. Qarnain, S. Muthuvel, S. Bathrinath, Review on government action plans to reduce energy consumption in buildings amid COVID-19 pandemic outbreak, Materials Today: Proceedings 45 (2021) 1264–1268.

[3] C. A. W. Ngouleu, Y. W. Koholé, F. C. V. Fohagui, G. Tchuen. Optimal sizing and techno-enviro-economic evaluation of a hybrid photovoltaic/wind/diesel system with battery and fuel cell storage devices under different climatic conditions in Cameroon ,Journal of Cleaner Production,423 (2023) 138753.

[4] I. Amoussou, E. Tanyi, L. Fatma, T. F. Agajie, I. Boulkaibet, N. Khezami, B. Khan. The optimal design of a hybrid solar PV/wind/hydrogen/lithium Battery for the replacement of a heavy fuel oil thermal power plant, Sustainability, 15 (2023) 11510.

[5] Z. Belboul, B. Toual, A. Kouzou, L. Mokrani, A. Bensalem, R. Kennel, M. Abdelrahem. Multiobjective optimization of a hybridPV/Wind/Battery/Diesel generator system integrated in microgrid: A case study in Djelfa, Algeria, Energies 15 no 10 (2022) 3579.

[6] A. S. Aziz, M. F. N. Tajuddin, T. E. K. Zidane, C. L. Su, A. J. K. Alrubaie, M. J. Alwazzan. Techno-economic and environmental evaluation of PV/diesel/battery hybrid energy system using improved dispatch strategy, Energy Reports,8 (2022), 6794-6814.

[7] A. B. Awan, M. Zubair, G. A. S. Sidhu, A. R. Bhatti, A. G. Abo-Khalil. Performance analysis of various hybrid renewable energy systems using battery, hydrogen, and pumped hydro-based storage units,

International Journal of Energy Research, 43 no 12 (2019), 6296-6321..

[8] A. A. Z. Diab, A. M. El-Rifaie, M. M. Zaky, M.A. Tolba. Optimal Sizing of Stand-Alone Microgrids Based on Recent Metaheuristic Algorithms, Mathematics, 10 no.1 (2022) 140.

[9] A. Pradhan, M. Marence, M. J. Franca. The adoption of Seawater Pump Storage Hydropower Systems increases the share of renewable energy production in Small Island Developing States, Renewable Energy, 177 (2021) ,448–460.

[10] E. T. Sayed, T. Wilberforce, K. Elsaid, M. K. H. Rabaia, M. A. Abdelkareem, K. J. Chae, A. G. Olabi, A critical review on environmental impacts of renewable energy systems and mitigation strategies: Wind, hydro, biomass and geothermal, Science of The Total Environment 766 (2021) 144505.

[11] M. H. Alsharif, R. Kannadasan, A. Y. Hassan, W. Z. Tawfik, M. K. Kim, M. A. Khan, A. A. A. Solyman, Optimization analysis of sustainable solar power system for mobile communication systems, Computers, Materials & Continua, 71 (2) (2022), 3244–3255.

[12] M. S. Gad, M. Said, A. Y. Hassan, Effect of different nanofluids on performance analysis of flat plate solar collector, Journal of Dispersion Science and Technology, 42 (12) (2021), 1867–1878.

[13] H. Shaban, E. H. Houssein, M. Pérez-Cisneros, D. Oliva, A. Y. Hassan, A. A. K. Ismaeel, D. S. AbdElminaam, S. Deb, M. Said, Identification of parameters in photovoltaic models through a Runge Kutta optimizer, Mathematics 9, (18) (2021) 2313.

[14] A. A. Teleb, M. R. Mahmoud, & G. M. Dousoky, PV-Based off Grid Valve Drive System for Leakage Protection in Water Networks. Journal of Advanced Engineering Trends, (2024).

[15] U. Sarma, S. Ganguly. Design optimization for component sizing using multi-objective particle swarm optimization and control of PEM fuel cell-battery hybrid energy system for locomotive application, IET Electrical Systems in Transportation,10 (2020), 52–61.

[16] A. M. Mohamed & Y. S. Mohamad, A Comparative Analysis on Different Techniques for Improving the PV System Performance Subjected to Variant Solar Irradiance. Journal of Advanced Engineering Trends, 43(2), (2024) 243-258.

[17] M. A. Mohamed, A. A. Z. Diab, Rezk. Partial shading mitigation of PV systems via different meta-heuristic techniques. Renewable energy, 130 (2019), 1159-1175.

[18] S. Rehman, H. U. R. Habib, S. Wang, M. S. Büker, L. M. Alhems, H. Z. Al Garni. Optimal design and model predictive control of standalone HRES: A real case study for residential demand side management. IEEE Access, 8 (2020), 29767-29814.

[19] A. Al-Ammar, H. U. R. Habib, K. M. Kotb, S. Wang, W. Ko, M. F. Elmorshedy, A. Waqar. Residential community load management based on optimal design of standalone HRES with model predictive control. IEEE Access, 8 (2020), 12542-12572.

[20] A. Acakpovi, P. Adjei, N. Nwulu, N. Y. Asabere. Optimal hybrid renewable energy system: A comparative study of wind/hydrogen/fuel-cell and wind/battery storage, Journal of Electrical and Computer Engineering, 2020, 1-15.

[21] A. Khan, N. Javaid. Optimal sizing of a stand-alone photovoltaic, wind turbine and fuel cell systems, Computers & Electrical Engineering, 85 (2020) 106682.

[22] A. A. Elbaset. Design, modeling and control strategy of PV/FC hybrid power system. J. Electrical Systems, 7(2) (2011), 270-286..

[23] F. S. Mahmoud, A. M. Abdelhamid, A. Al Sumaiti, A. H. M. El-Sayed, A. A. Z. Diab. Sizing and Design of a PV-Wind-Fuel Cell Storage System Integrated into a Grid Considering the Uncertainty of Load Demand Using the Marine Predators Algorithm, Mathematics, 10 (19) (2022) 3708.

[24] R. J. Rathish, K. Mahadevan, S. K. Selvaraj, J. Booma. Multi-objective evolutionary optimization with genetic algorithm for the design of off-grid PV-wind-battery-diesel system. Soft Computing, 25 (2021), 3175-3194

[25] A. Maleki, F. Pourfayaz, Optimal sizing of autonomous hybrid photovoltaic/wind/battery power system with LPSP technology by using evolutionary algorithms, Solar Energy, 115 (2015), 471–483.

[26] M. J. Hadidian-Moghaddam, S. Arabi-Nowdeh, M. Bigdeli. Optimal sizing of a stand-alone hybrid photovoltaic/wind system using new grey wolf optimizer considering reliability. Journal of Renewable and Sustainable Energy, 8(3) (2016).

[27] M. Bilal, I. Alsaidan, M. Alaraj, F. M. Almasoudi, M. Rizwan. Techno-economic and environmental analysis of grid-connected electric vehicle charging stations using ai-based algorithm. Mathematics, 10(6) (2022) 924.

[28] C. Ghenai, T. Salameh, & A. Merabet, Technico-economic analysis of off grid solar PV/Fuel cell energy system for residential community in desert region. International Journal of Hydrogen Energy, 45(20), (2020) 11460-11470.

[29] A. A. Z Diab, S. I. El-ajmi, H. M. Sultan, Y. B. Hassan. Modified farmland fertility optimization algorithm for optimal design of a grid-connected hybrid renewable energy system with fuel cell storage: Case study of Ataka, Egypt. International Journal of Advanced Computer Science and Applications, 10 (8), 119-132.

[30] H. M. Sultan, A. S. Menesy, S. Kamel, A. Korashy, S. A. Almohaimeed, & M. Abdel-Akher, An improved artificial ecosystem optimization algorithm for optimal configuration of a hybrid PV/WT/FC energy system. Alexandria Engineering Journal 60 (1), (2020) 1001–1025.

[31] A. Khan & N. Javaid, Optimal sizing of a stand-alone photovoltaic, wind turbine and fuel cell systems.

Computers & Electrical Engineering, (85), 106682 (2020).

[32] A. C. Duman, & Ö. Güler, Techno-economic analysis of off-grid PV/wind/fuel cell hybrid system combinations with a comparison of regularly and seasonally occupied households. Sustainable Cities and Society, (42), (2018) 107-126.

[33] M. J. Hadidian Moghaddam, A. Kalam, S. A. Nowdeh, A. Ahmadi, M. Babanezhad & S. Saha, Optimal Sizing and Energy Management of Stand-alone Hybrid Photovoltaic/Wind System Based on Hydrogen Storage Considering LOEE and LOLE Reliability Indices Using Flower Pollination Algorithm. Renewable Energy ,(135) (2018), 1412–1434.

[34] https://bluebirdsolar.com/products/bluebird-5kw-solar-panels.

[35] https://www.taqetna.com/wp-content/uploads/2020/06/REYAH50-Wind-Turbine-Datasheet.pdf

[36] https://hyfindr.com/marketplace/components/fuelcell-stacks/pem-stacks/fuel-cell-stack-eh-81-100-kw/

[37] S. Moghaddam, M. Bigdeli, M. Moradlou, P. Siano. Designing of stand alone hybrid PV/wind/battery system using improved crow search algorithm considering reliability index, International Journal of Energy and Environmental Engineering, 10 (2019), 429–449.

[38] T. Ma, H. Yang, L. Lu, A feasibility study of a stand-alone hybrid solar–wind–battery system for a remote island, Applied Energy, 121 (2014), 149–158.

[39] Hassan, A. Y., Soliman, A. M., Ahmed, D., & Saleh, S. M. (2022). Wind cube optimum design for wind turbine using meta-heuristic algorithms. Alexandria Engineering Journal, 61(6), 4911-4929.

[40] S. Ott, A. Orfanidi, H. Schmies, B. Anke, H. N. Nong, J. Hübner, U. Gernert, M. Gliech, M. Lerch, P. Strasser. Ionomer distribution control in porous carbon-supported catalyst layers for high-power and low Pt-loaded proton exchange membrane fuel cells. Nature materials, 19 (2020), 77-85.

[41] M. K. Singla, P. Nijhawan, A. S. Oberoi. Hydrogen fuel and fuel cell technology for a cleaner future: A review. Environmental Science and Pollution Research, 28 (2021), 15607–15626.

[42] M. K Singla, P. Nijhawan, A. S. Oberoi. Parameter estimation of proton exchange membrane fuel cell using a novel meta-heuristic algorithm. Environmental Science and Pollution Research, 28 (2021) 34511-34526.

[43] M. K Singla, P. Nijhawan, A. S. Oberoi. Cost–benefit comparison of fuel cell-based and battery-based renewable energy systems. International Journal of Energy Research, 46(2) (2022), 1736-1755.

[44] E. Trojovská, M. Dehghani, P. Trojovský. Zebra optimization algorithm: A new bio-inspired optimization algorithm for solving optimization algorithm. IEEE Access, 10 (2022) 49445-49473.

[45] NASA Surface meteorology and solar energy; Available from: http://eosweb.larc.nasa.gov/sse/.